ACS APPLIED POLYMER MATERIALS

pubs.acs.org/acsapm
Article

Evidence of Positive Cooperativity in the Binding Behavior of Molecularly Imprinted Polymers Prepared by Solid Phase Polymerization Synthesis

Valentina Testa, Laura Anfossi, Simone Cavalera, Fabio Di Nardo, Thea Serra, and Claudio Baggiani*

Cite This: ACS Appl. Polym. Mater. 2025, 7, 3286−3295
Read Online

ABSTRACT: Nanosized molecularly imprinted polymers (nanoMIPs) and polyclonal antibodies are assumed to share the same binding behavior due to the presence of mutually independent binding sites and characterized by a continuous distribution of the binding affinity with respect to an average value. This gives rise to a convex Scatchard plot and is well described by the Langmuir−Freundlich (Sips) isotherm. Nevertheless, some preliminary experimental indications suggest the possibility of a different binding behavior, characterized by positive cooperativity. Since this behavior would have significant repercussions on the practical use of nanoMIPs, the binding behavior of a nanoMIP with molecular recognition properties toward ciprofloxacin has been thoroughly investigated. Repeated equilibrium binding experiments on nanoMIPs of different cross-linking degrees (2%, 10%, and 20% molar of methylene-bis-acrylamide as cross-linker, respectively) allowed to accurately determine the binding isotherms over a wide range of ligand concentrations. The consequent statistical treatment of the data showed the clear prevalence of binding isotherm models consistent with positive cooperativity (heterogeneity parameter $n > 1$ and concave Scatchard plot) when compared to other alternative binding models considered. Moreover, the exponential heterogeneity parameter does not correlate with the degree of cross-linking of the nanoMIPs, suggesting that the origin of positive cooperativity could be due not only to the degree of stiffness of the nanopolymer but also to the structural proximity of the binding sites, as shown by further experimental data obtained from nanoMIPs prepared with rabbit γ-globulins, a much bulkier template than ciprofloxacin.

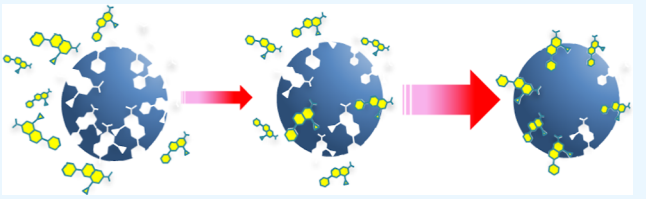

KEYWORDS: *molecularly imprinted polymer, nanoMIP, binding isotherm, Langmuir−Freundlich isotherm, binding cooperativity*

INTRODUCTION

Molecularly imprinted polymers (MIPs) owe their peculiar molecular recognition properties to nanocavities formed during the polymerization process, following the presence of template molecules and appropriate functional monomers in the prepolymerization mixture.[1,2] Such nanocavities can be considered, in all respects, as binding sites, the dimension and shape of which are complementary to those of the template, and where the molecular recognition mechanism is based on noncovalent interactions between the template, or similar molecular structures, and the binding site, in accordance with the "key and lock" principle. For this reason, MIPs have long been defined as synthetic analogues of natural antibodies.[3−5] It follows that, as mimics of the latter, the binding behavior can be considered identical so long as they show well-defined binding thermodynamics and kinetics.[6−8]

In a striking analogy with natural antibodies present in polyclonal antisera, MIPs prepared using a noncovalent imprinting approach are characterized by a multiplicity of binding sites with a wide and continuous distribution of affinities toward the template.[9,10] This "polyclonal" feature is well described by the Langmuir−Freundlich (Sips) eq (Chart 1).[11] In this model, the relationship between the free (F) and bound (B) ligand concentrations depends from three parameters, which have physical meaning: the apparent equilibrium binding constant, K_{eq} (corresponding to the median value of the equilibrium binding constants associated with the binding sites), the binding site density, B_{max}, and the heterogeneity index, n, an exponent term whose numerical value is between 0 and 1, with $n = 1$ for MIPs with a "monoclonal" binding behavior where all the binding sites have the same equilibrium binding constant.[12,13] However, note that the heterogeneity index can be conceived in a different way. Indeed, by removing the upper limit equal to unity for n, the Langmuir−Freundlich isotherm takes the form of the Hill equation, which describes binding systems exhibiting cooperativity.[14] In a broader vision, with $n > 1$, there is positive cooperativity, i.e., the binding of further ligand molecules to

Received: December 19, 2024
Revised: February 12, 2025
Accepted: February 17, 2025
Published: February 22, 2025

Chart 1. Relationships between isotherm models considered in this work. $\theta = B/B_{max}$, K_{eq} is the apparent equilibrium binding constant, B_{max} is the total binding site density, n and m are the heterogeneity parameters, and a is an empirical parameter, which appear in Freundlich and Henry models. Red color: models considered in this work. Dashed arrows: valid when $K_{eq}F \ll 1$ only.

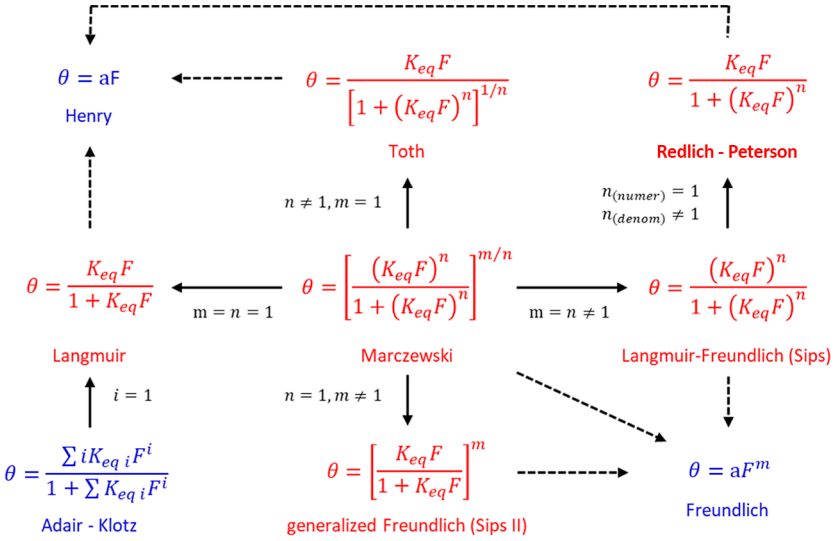

the ligand−receptor complex is favored, while with $n = 1$, there is no cooperativity, and with $n < 1$, there is negative cooperativity, i.e., the binding of further ligand molecules to the ligand−receptor complex is unfavored.[15] In the latter case, supposing equilibrium conditions, the occupation of the binding sites by increasing amounts of ligand starts from the binding sites characterized by the highest affinity to proceed toward saturation through occupation of binding sites increasingly less affine, a process that can be interpreted both as negative cooperativity and as an effect of binding heterogeneity.

Natural antibodies show binding cooperativity between Fab binding sites in very particular conditions only, typically when the antigen is a multivalent macromolecule characterized by multiple repeated epitopes in its structure.[16] Likewise, positive cooperativity in MIPs has been described only for the binding of molecular clusters stabilized by ligand−ligand interactions.[17,18] As a significant example, this is the case of a bilirubin-imprinted polymer whose isotherm presented the typical sigmoidal shape characteristic of a binding behavior with positive cooperativity.[19] However, it is generally assumed that in the absence of templates characterized by such peculiar properties, MIPs cannot present positive cooperativity but only negative cooperativity effects (i.e., binding heterogeneity) and, consequently, the binding behavior can be appropriately well described by a Langmuir−Freundlich isotherm model with $n < 1$.[7] The lack of observed positive cooperativity can be explained by the steric rigidity of the binding sites obtained by molecular imprinting. In fact, in order to ensure the structural stability of the binding sites essential for maintaining molecular recognition, the typical composition of the prepolymerization mixtures includes a significant amount of cross-linking monomer, generally set between 70 and 90 mol %.[20]

Imprinted nanogels (nanoMIPs) have recently gained attention due to their interesting properties such as improved binding sites accessibility, faster binding kinetics, reduced nonspecific binding, and enhanced biocompatibility.[21−23] Although nanoMIPs can be prepared through different polymerization techniques, such as microemulsion or solid phase synthesis,[24−26] they differ from traditional MIPs in the composition of the prepolymerization mixture because the cross-linking agent is present in limited quantities compared to the functional monomers, typically never above 2 mol %. As it is reasonable to assume that the steric rigidity of the polymeric structure of nanoMIPs is much lower than that of traditional MIPs, binding behavior with positive cooperativity cannot be excluded a priori. Thus, a careful examination of the experimental binding isotherm corresponding to the interaction between a nanoMIP and its template ligand must be able to confirm or deny this hypothesis.

A qualitative criterion that marks the possibility of cooperativity effects concerns the shape of the binding isotherm when converted in the Scatchard plot, i.e., the bound vs free data are converted in bound to free ratio vs bound. Although it is not convenient to fit the transformed data to obtain the numerical values of the binding parameters,[27−29] the appearance of a concave plot indicates the presence of a positive cooperativity effect, just as a convex plot indicates the presence of a negative cooperative effect or binding heterogeneity.[15] However, to confirm the presence of positive cooperativity, it is necessary to fit the experimental data by using an appropriate isotherm model. As mentioned before, a binding system characterized by cooperativity effects is described by a more complex model than a simple Langmuir isotherm, and that this model does not necessarily have to coincide with the Langmuir−Freundlich isotherm, as it is known that this isotherm is only one of many describing complex binding behaviors.[30] The choice of the appropriate model is still hindered by the fact that the vast majority of the numerous models reported in the literature are empirical or semiempirical, and therefore, there is no direct relationship between the model parameters and the mechanism on which the ligand−receptor interaction depends for the system studied. Therefore, excluding a priori totally empirical models, it is opportune to consider a set of semiempirical equations correlated to the well-known Adair-Klotz model, which explicitly describes systems characterized by cooperative effects

https://doi.org/10.1021/acsapm.4c03726
ACS Appl. Polym. Mater. 2025, 7, 3286−3295

with a sounding theoretical foundation.[15,31] It is easy to see that this set of models is an extension of the simple Langmuirian equation too, and it is characterized by the presence of one or more exponential terms.[32,33] In fact, as illustrated in Chart 1, it starts from the Marczewski model characterized by the presence of two different heterogeneity indices and assigning at the heterogeneity indices (m, n). Then, assigning at these indices values of >1, <1, or 1, it is possible to obtain a series of simplified models corresponding, respectively, to the well-known Langmuir,[34] Redlich-Peterson,[35] Langmuir−Freundlich (Sips),[11] Generalized Freundlich (Sips II),[36] and Toth isotherms.[37] Furthermore, assuming that the $K_{eq}F$ product takes on values significantly lower than unity (which happens in conditions far from the saturation of the binding sites by the ligand), the equations simplify, becoming, respectively, the Freundlich isotherm (from the Langmuir−Freundlich, Generalized Freundlich, and Marczewski isotherms) and the Henry isotherm (from Langmuir, Redlich-Peterson, and Toth isotherms). Therefore, in the presence of positive cooperativity, all models compatible with this and showing a convex Scatchard plot (Langmuir−Freundlich, Generalized Freundlich, and Marczewski) must fit the experimental isotherm significantly better than models that do not show a convex Scatchard plot (Langmuir, Freundlich, Redlich-Peterson, and Toth).

Herein, to experimentally confirm this possibility, we studied the binding properties of a nanoMIP imprinted against ciprofloxacin at three cross-linking levels (2%, 10%, and 20% molar, respectively) prepared by solid-phase polymerization synthesis, which have been previously described by our laboratory.[38,39] The experimental binding isotherms were measured through equilibrium partition measurements performed in an aqueous buffer at pH 7.4, and the binding data were fitted with the set of isotherm binding models reported in Chart 1. It can be anticipated that models with the best fit were found to be those presenting a sigmoidal shape, thus envisaging positive cooperativity, while simpler models that exclude this type of behavior were found not suitable to correctly describe the experimental data.

EXPERIMENTAL SECTION

Materials. Acrylic acid (AA), ammonium persulfate (APS), ciprofloxacin, diisopropylcarbodiimide (DIC), *N*-hydroxysuccinimide (NHS), *N*-isopropylacrylamide (NIPAm), *N*,*N*′-methylene-bis-acrylamide (BIS), *N*-*tert*-butylacrylamide (TBAm), and *N*,*N*,*N*′,*N*′-tetramethylethylenediamine (TEMED) were purchased from Sigma-Merck (Milan, Italy). Ultrapure water was obtained with a Purelab Prima System from Elga (Marlow, UK). Ligand stock solutions were prepared by dissolving 25 mg of ciprofloxacin in 25 mL of phosphate buffer (20 mmol L^{-1}, pH 7.4) and stored in the dark at −20 °C for no more than a week, after which they were discarded.

Synthesis of nanoMIPs. Prepolymerization mixtures (overall monomer concentration: 1.3 mmol L^{-1}) were prepared by mixing cross-linker and functional monomers (molar ratio BIS/AA/NIPAM/TBAm = 2:20:30:48 for 2% cross-linked nanoMIP, 10:18:28:44 for 10% cross-linked nanoMIP, and 20:16:24:40 for 20% cross-linked nanoMIP, respectively) in 25 mL of ultrapure water. Then, 5 mL of mixture was introduced into 50 mL polypropylene SPE cartridges filled with 2.5 g of glass beads (Spheriglass-2429, 53−106 μm average particle size, Potters, UK) covalently grafted with ciprofloxacin as previously reported.[36] The cartridges were deoxygenated by sparging with nitrogen for 5 min; then, 3 μL of TEMED and 100 μL of 30 mg mL^{-1} aqueous solution of APS were added to the sealed cartridges with a syringe, and polymerization was carried out at room temperature for 60 min in a roller-equipped incubator. The supernatant was eliminated by vacuum aspiration, cartridges were cooled to 4 °C, and low affinity nanoMIPs (including those with low intrinsic affinity as well as those with few binding sites) and polymerization byproducts were washed with 10 × 2 mL of ice-cold water. High affinity nanoMIPs were recovered by eluting the cartridges at room temperature with 5 × 2 mL of 0.1 mol L^{-1} formic acid. The eluates were dried under a vacuum, weighed, and stored at room temperature. NanoMIPs were covalently grafted onto aminated glass beads in accordance with the protocol previously reported with minor modifications.[38] In 4 mL glass vials, 1 mg of nanoMIPs was dissolved under sonication in 1 mL of *N*,*N*-dimethylformamide. Then, 5 mg of NHS (0.043 mmol) and 7 mg of DIC (0.047 mmol) were added, and the solution was incubated at 4 °C for 2 h. Then, it was transferred into a 10 mL flask containing 1 g of aminated glass beads in 4 mL of phosphate buffer (0.1 mol L^{-1}, pH 7.4). The suspension was incubated at room temperature overnight, filtered on a 0.22 μm nylon membrane, washed with ultrapure water, rinsed twice with acetone, dried under vacuum at room temperature, and stored in the dark at 4 °C.

HPLC Method. Reverse phase high-performance liquid chromatography (HPLC) analysis was used for ciprofloxacin determination. The HPLC apparatus (Merck-Hitachi, Milan, Italy) was a LaChrom Elite system composed of a programmable binary pump L-2130, an autosampler L-2200, and a fluorescence detector L-7485, provided with EZChrom Elite software for the instrumental programming, data acquisition, and data processing. The column used was a 100 × 4.6 mm C-18 Onyx column (Phenomenex, Milan, Italy). The mobile phase was water/acetonitrile 85 + 15, formic acid 0.5% (v/v). Elutions were performed in isocratic conditions at a flow rate of 0.7 mL min^{-1}. The sample volume injected was 25 μL, and the fluorescence wavelengths were λ_{ex} = 280 and λ_{em} = 440 nm. Ciprofloxacin working solutions between 1 and 275 ng mL^{-1} were prepared in phosphate buffer (20 mmol L^{-1}, pH 7.4) immediately before use. The solutions were analyzed in triplicate, and mean peak areas were plotted against ciprofloxacin concentrations. Calibration plots were drawn by weighted linear regression (weight = 1/conc). As the experimental binding isotherms were obtained by different sets of equilibrium partition data, for each run of measurements, a new calibration plot was traced.

Experimental Binding Isotherms. The binding isotherms were obtained by repeated equilibrium partition experiments. For each set of measures, about 40 mg of glass beads supporting nanoMIPs was exactly weighed in 4 mL flat bottom amber glass vials. Then, 1.0 mL of phosphate buffer (20 mmol L^{-1}, pH 7.4) containing increasing amounts of ciprofloxacin ranging from 5 to 275 ng was added. The vials were incubated overnight at room temperature under continuous agitation on a horizontal rocking table. Then, the solutions were filtered on 0.22 μm nylon membranes, and the free amounts of ciprofloxacin (μmol L^{-1}) were measured by HPLC analysis. Bound ciprofloxacin (nmol g^{-1} of glass beads) was obtained by subtracting the free ciprofloxacin from the total and scaling for the glass beads weight. Each experimental point was assessed as the average of 10−30 repeated measures, discarding data exceeding the mean value ±1.96 standard deviations. For each binding isotherm model considered, the binding parameters were calculated with TableCurve 2D 5.0 (Systat Software Inc., Richmond, CA, USA) using nonlinear robust least-squares fitting based on Levenberg−Marquardt algorithm with Pearson VII limit minimization. To avoid being trapped in local minima, fitting was carried out several times by using different initial guess values for the binding parameters. The prediction coefficient, Q^2, was calculated as

$$Q^2 = 1 - \frac{\mathrm{PRESS}}{\mathrm{TSS}}$$

where PRESS is the predictive residual error sum of squares, defined as the sum of the squares of the prediction errors obtained by omitting one experimental point at a time and refitting the model each time,[40] and TSS the total sum of squares. The Bayesian information criterion (BIC) was calculated as

https://doi.org/10.1021/acsapm.4c03726
ACS Appl. Polym. Mater. 2025, 7, 3286−3295

$$\mathrm{BIC} = \ln \mathrm{SSE} + \frac{k}{N}\ln N$$

where k is the number of parameters in the model, N is the number of data points, and SSE is the sum of squared estimate of errors.[41]

RESULTS AND DISCUSSION

Experimental Binding Isotherms. In determining the binding isotherms by equilibrium partition experiments, a major source of uncertainty in the data arises from the fact that it is very difficult to independently measure both the free and bound fractions of the ligand. In the specific case of the experiments reported here, HPLC was used to measure the free fraction but obviously not the bound one, which was therefore determined indirectly by subtracting the free fraction from the total amount of ligand placed at equilibrium. It follows that the error associated with the free fraction is propagated to the bound fraction. A second but no less important reason for uncertainty lies in the fact that, from a preliminary examination of the experimental data obtained in the past for nanoMIP imprinted against ciprofloxacin,[38,39] we speculated that the cooperative effect, if present, must manifest itself as a sigmoidal inflection present at relatively low doses of ligand compared to those of saturation of the binding sites, i.e., for low concentrations of free ligand at equilibrium that are difficult to measure with adequate precision. For these two reasons, we decided to measure the experimental binding isotherms using a high (>20) number of data points replicated between 10 and 20 times each in a concentration range centered on the region in which the presence of the inflection in the binding curve could be presumed.

The experimental binding isotherm and the corresponding Scatchard plots measured for ciprofloxacin on nanoMIP cross-linked at 2%, 10%, and 20% are reported in Figures 1 and 2,

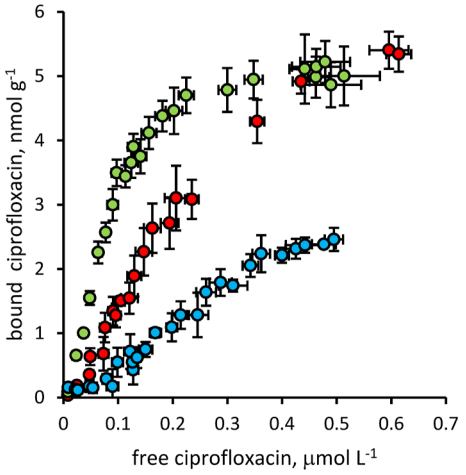

Figure 1. Experimental binding isotherms for ciprofloxacin and nanoMIPs cross-linked at 2% (red dot), 10% (green dots), and 20% (blue dots). Error bars: ± 1σ. Bound ciprofloxacin must be intended as nmol × g of glass beads.

respectively. A sigmoidal inflection located at approximately 0.05−0.2 μmol L^{-1} of free ligand is visible for all three binding isotherms, while the corresponding Scatchard plots show a pronounced downward concavity for all three sets of measurements, with maxima located approximately between 1 and 4 nmol g^{-1} of bound ligand. As expected, despite the uncertainty due to the propagation of the experimental error,

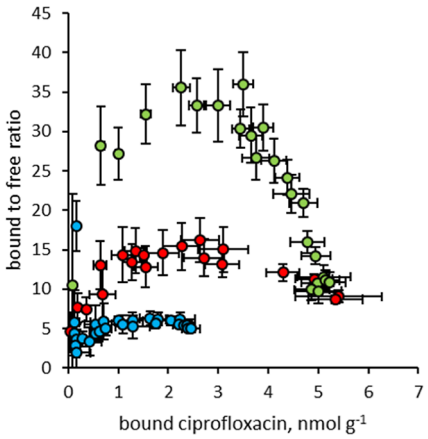

Figure 2. Scatchard plots for ciprofloxacin and nanoMIPs cross-linked at 2% (red dot), 10% (green dots), and 20% (blue dots). Error bars: ± 1σ. Bound ciprofloxacin must be intended as nmol × g of glass beads.

the distributions of the experimental points in the binding isotherms and in the Scatchard plots show that a simple isotherm model such as Langmuir cannot correctly describe these data and that more complex models are needed.

Selection of the Binding Isotherm Models. The fit of the experimental data with the set of isotherm models considered in this work is reported on a semilogarithmic scale in Figure 3. It confirms the inadequacy of a simple model like Langmuir's to reproduce correctly the trend of the experimental data when the inflection is present, namely, for low concentrations of free ligand, <0.06 μmol L^{-1}, while more complex models reproduce the trend of the experimental data well in the entire measured range of free ligand concentrations.

A first step concerning the ability of the various models to correctly represent the experimental binding data can be made by examining the Scatchard plots reported in Figure 4. It must be noted that, due to the infeasibility of converting the binding models according to the Scatchard transformation, the curves were not obtained by directly fitting the transformed binding data but by numerically transforming the curves corresponding to the bound vs free models. In this case, it is overly complex to obtain either the parameters of the resulting equations or the corresponding fit statistics, but it is possible to visually observe that not only does the simple Langmuir model, as expected, not show the convex shape characteristic of Scatchard plots in positive cooperativity conditions, but also more complicated models, such as Redlich-Peterson and Toth have shapes far from the pattern described by the transformed experimental data and, in the latter case, are physically impossible. On the contrary, models compatible with positive cooperativity (Langmuir-Freundlich, Generalized Freundlich, and Marczewski) show a very good correspondence between the shape of the curves and the distribution of such experimental binding data, leading to the conclusion that only the latter must actually be taken into consideration when appropriately describing the experimental data.

For all the set of models considered, the fit statistics reported in Table 1 show a determination coefficient (r^2) higher than 0.950, but, nevertheless, considering the standard error of the estimate (SEE) and the residual sum of the squares (RSS) values, it is quite clear that the models can be divided into three distinct groups: a first group includes the binding isotherm models, which describe correctly the corresponding

https://doi.org/10.1021/acsapm.4c03726
ACS Appl. Polym. Mater. 2025, 7, 3286−3295

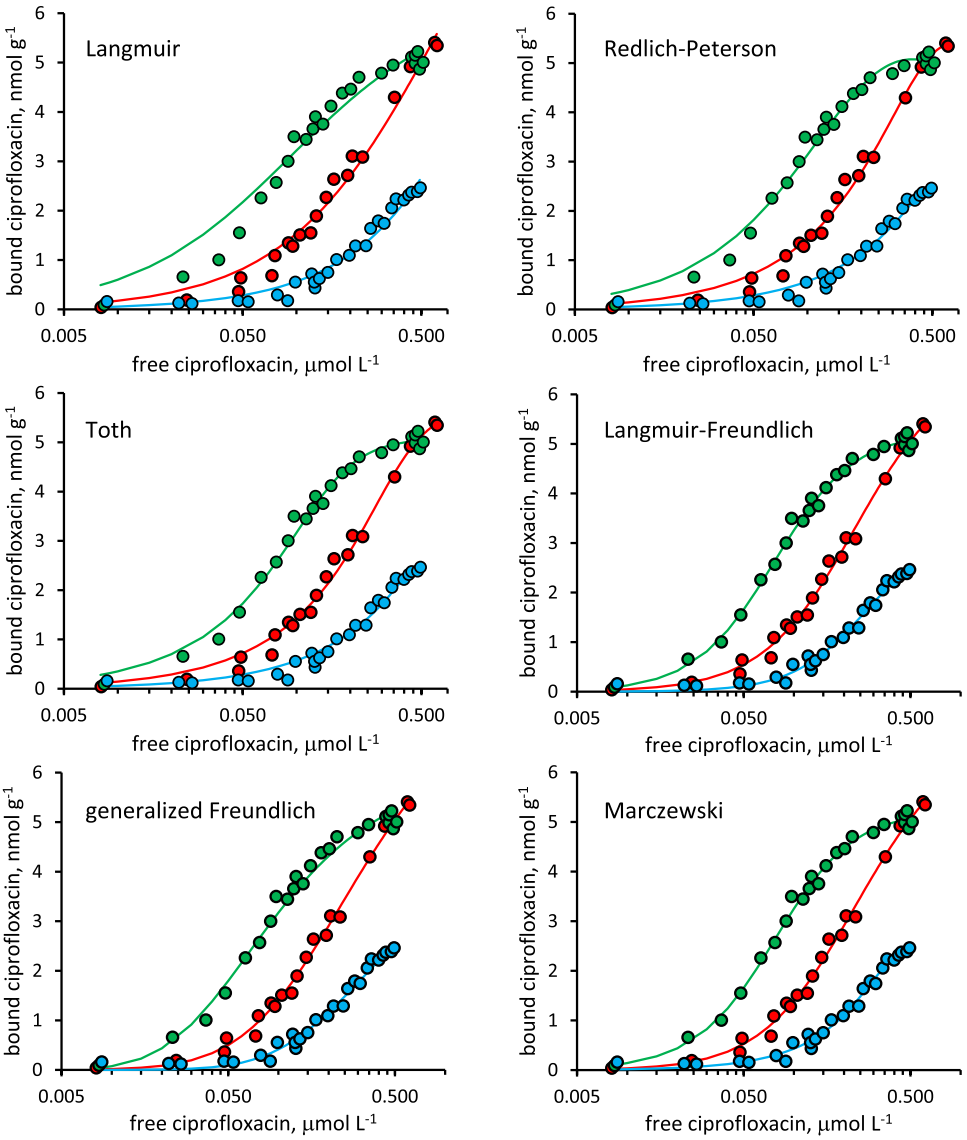

Figure 3. Binding isotherm models fitting the experimental data for ciprofloxacin−nanoMIP 2% (red), ciprofloxacin−nanoMIP 10% (green), and ciprofloxacin−nanoMIP 20% (blue). Error bars omitted for greater clarity. Bound ciprofloxacin must be intended as nmol × g of glass beads.

Scatchard plots (Langmuir−Freundlich, Generalized Freundlich, and Maczewski models), characterized by r^2 values higher than 0.980 and SSE and RSS values markedly lower than 0.145 and 0.345, respectively (with the exception of the Generalized Freundlich model fitting the data for nanoMIP 10%, which shows an anomalous RSS value of 0.705), indicating an excellent fit of the experimental data. A second group includes the Redlich−Peterson and Toth models, characterized by r^2 values between 0.973 and 0.988, thus comparable to the first group, but with SSE values in the range 0.136−0.184 and RSS values in the range 0.447−0.713, significantly higher than the first group and indicating a fit to the experimental data of lower quality. Finally, the Langmuir model, which must be considered separately since it is characterized by the lowest r^2 values and with SSE and RSS values markedly higher, confirms that this model is much less suitable in representing the experimental data than all the others considered in this work.

Concerning the prediction coefficient, Q^2, it is no coincidence that the values calculated retrace the pattern observed in the case of r^2 values, as they are two similar statistical indicators, but since Q^2 derives from the PRESS statistic that is calculated by refitting the model after omitting one experimental point at a time, it also provides a direct estimate of the robustness of the models with respect to changing experimental data, confirming that Redlich-Peterson and Toth models are less suitable to describe the binding isotherm as they are more sensitive to random variations in the experimental data. A remarkable exception is represented by the Generalized Freundlich model, fitting the data for nanoMIP 10%, which shows a low value of 0.955 for Q^2. The nature of this anomaly, however, can be easily explained by the fact that the validation process was particularly difficult, showing a tendency for this model to show substantial instability when single experimental points were omitted from the fit. Thus, considering the models with the best statistics and with a Scatchard plot presenting concavity (Langmuir−Freundlich, Generalized Freundlich, and Marczewski), it is clear that although there are differences between such models, the fit statistics could be still considered indicative of a wholesome good fit of the experimental data

https://doi.org/10.1021/acsapm.4c03726
ACS Appl. Polym. Mater. 2025, 7, 3286−3295

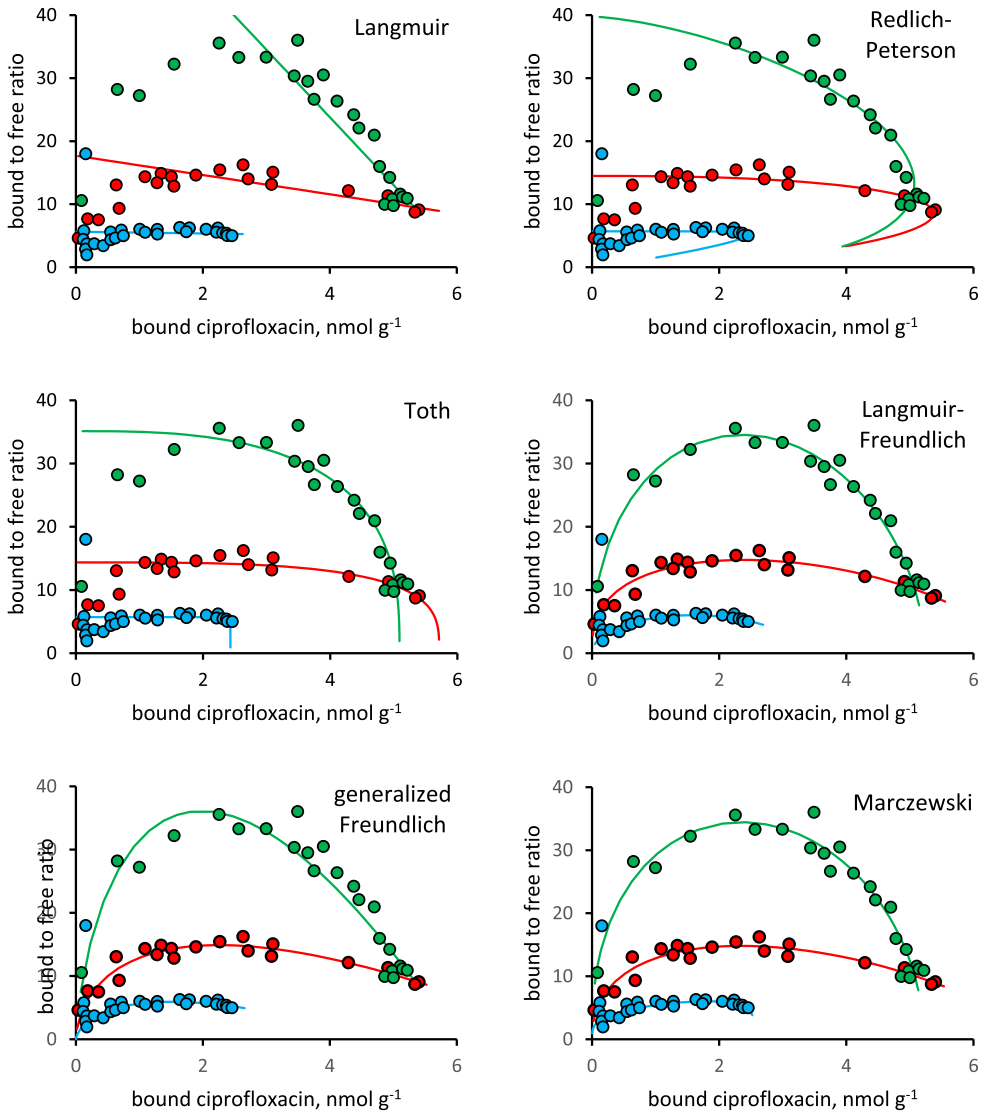

Figure 4. Scatchard plots and transformed binding isotherm models for ciprofloxacin−nanoMIP 2% (red), ciprofloxacin−nanoMIP 10% (green), and ciprofloxacin−nanoMIP 20% (blue). Error bars omitted for greater clarity. Bound ciprofloxacin must be intended as nmol × g of glass beads.

and therefore insufficient to effectively discriminate one model from another if taken alone.

An in-depth look at the binding parameters calculated for the models and reported in Table 2 shows that some of these parameters present values anomalously high and are affected by a severe uncertainty, with calculated Student's *t*-values (probability level $p = 0.05$) well below those tabulated. In particular, while the Langmuir−Freundlich model does not show anomalous parameters in any case, the Generalized Freundlich model presents anomalous values for the apparent equilibrium binding constant in the case of the nanoMIP 10%—confirming what was said previously for this case regarding the anomalous value of PRESS—and for the heterogeneity index and the apparent equilibrium binding constant for the nanoMIP 20%, while the Marczewski model presents anomalous values for the first (of two) heterogeneity indexes in the case of the nanoMIP 20%. These uncertainties lead to the conclusion that although all three models seem to describe the experimental data well, the Langmuir−Freundlich model is substantially more reliable than the others. This is also confirmed by the calculated values of the BIC. Weighing the SSE for the number of data points (N) and the number of parameters in the model (k), it represents a powerful tool to obtain direct information about the quality of a model and, given a set of models, to estimate the quality of each model when compared to the other models.[41] In Table 3, it is possible to see that for the three nanoMIPs, the most negative BIC value corresponds to the Langmuir−Freundlich model, which therefore turns out to be the optimal model. Compared to the Langmuir−Freundlich model, the remaining models show progressively increasing ΔBIC values with a trend in agreement both with the statistical parameters reported in Table 1 and with the parameter values of the models reported in Table 2. Moreover, as ΔBIC values larger than 3 are distinctive of statistically different models,[42] once again the Langmuir, Redlich-Paterson, and Toth models appear not to be representative of the experimental data, while the other models are so to a limited extent only, i.e., in the case of nanoMIP 2% (Generalized Freundlich) and nanoMIP 20% (Marczewski).

Effect of Cross-Linking on Cooperativity. As stated in the introduction, cooperativity effects in the binding behavior

https://doi.org/10.1021/acsapm.4c03726
ACS Appl. Polym. Mater. 2025, 7, 3286−3295

Table 1. Statistics of the Binding Isotherm Models[a]

	model	r^2	SSE	RSS	PRESS	Q^2
nanoMIP 2%	Langmuir	0.977	0.248	1.104	1.427	0.974
	Redlich-Peterson	0.988	0.183	0.568	0.677	0.988
	Toth	0.988	0.180	0.552	0.681	0.988
	Lang. Freund	0.993	0.141	0.338	0.467	0.991
	Gen. Freundlich	0.993	0.142	0.342	0.479	0.991
	Marczewski	0.992	0.144	0.335	0.510	0.991
nanoMIP 10%	Langmuir	0.954	0.320	2.260	2.554	0.953
	Redlich-Peterson	0.985	0.184	0.713	0.895	0.983
	Toth	0.989	0.155	0.508	0.645	0.988
	Lang. Freund	0.994	0.120	0.305	0.401	0.993
	Gen. Freundlich	0.995	0.110	0.705	2.458	0.955
	Marczewski	0.993	0.123	0.305	0.510	0.991
nanoMIP 20%	Langmuir	0.966	0.154	0.590	0.735	0.961
	Redlich-Peterson	0.973	0.138	0.454	0.554	0.971
	Toth	0.973	0.136	0.447	0.497	0.974
	Lang. Freund	0.985	0.103	0.254	0.315	0.983
	Gen. Freundlich	0.983	0.110	0.288	0.358	0.981
	Marczewski	0.986	0.099	0.227	0.301	0.984

[a] r^2: determination coefficient corrected for model's degrees of freedom; SSE: standard error of the estimate; RSS: residual sum of squares; PRESS: predictive residual error sum of squares; and Q^2: prediction coefficient.

of nanoMIPs can hypothetically be related to the low degree of cross-linking, which guarantees flexibility of the polymer structure clearly superior to that of MIPs prepared using traditional techniques. It follows that as the degree of cross-linking increases, the nanoMIPs stiffness must progressively increase, and, consequently, the binding properties can change, with cooperative effects becoming gradually less observable, i.e., the heterogeneity (i.e., cooperativity) parameter, n, in the binding isotherm model must tend to a value close to or lower than unity.

Nevertheless, the experimental results here reported show that as the cross-linking degree increases, the heterogeneity parameter for the Langmuir−Freundlich model reported in Table 2 does not decrease at all, but on the contrary, shows a substantial stability with values statistically indistinguishable from each other (p = 0.05, nanoMIP 2%—nanoMIP 10% t = 1.86, nanoMIP 2%—nanoMIP 20% t = 1.82, nanoMIP 10%—nanoMIP 20% t = 1.82) of 1.57 ± 0.10 (nanoMIP 2%), 1.82 ± 0.09 (nanoMIP 10%), and 1.96 ± 0.19 (nanoMIP 20%), respectively. In the absence of experimental information on the actual stiffness of the polymer chains in the nanoMIP particles, it is therefore difficult to justify this absence of a relationship between cooperativity and nanogel structure, unless we admit that the increase of the cross-linking from 2% to 20% does not substantially impact the overall stiffness of the nanogels and, consequently, is unable to influence the cooperative binding behavior.

Alternatively, if the stiffness of the polymer chains increases substantially with increasing degree of cross-linking, it is yet possible that the positive cooperativity is preserved mainly due to proximity effects of kinetic or steric nature between binding sites. Obviously, in this scenario, it is necessary that a high number of binding sites adjacent to each other will be present in the nanoMIPs. In this regard, we performed some elementary calculations on the possible distance of the binding sites, based on their surface density determined by the study of the binding isotherms. These calculations, detailed in the Supporting Information, indicate that the average distance between one binding site and another is in a range of 4−6 nm (4.4 nm for nanoMIP 2%, 4.9 nm for nano MIP 10%, and 6.2 nm for nanoMIP 20%), suggesting the reasonableness of the hypothesis of a large number of binding sites very close to each other and therefore capable of interacting mutually.

A further indirect evidence that the binding cooperativity may be due to proximity effects consists in the binding isotherms obtained on rabbit γ-globulins-binding nanoMIPs prepared at increasing degrees of cross-linking and published by us recently.[43] In this case, the increase of the cross-linking degree from 1% to 20% results in a decrease in the binding sites density and a marked increase in the apparent equilibrium binding constants, confirming the results reported here, but without any trace of cooperative behavior. In fact, the Scatchard plots corresponding to the published binding isotherms (Figure 5) do not show any convexity but, on the contrary, are straight lines across the entire experimental range of binding data. In this case, the absence of cooperativity can be explained if we assume that the latter depends on the proximity effects. In fact, γ-globulins are macromolecules much larger than fluoroquinolones, capable of exerting a considerable steric hindrance in the formation of the cross-linked polymer during the template process, and it is therefore reasonable to think that the binding sites generated by a sterically bulky template result considerably distant from each other and therefore not capable of mutually influencing.

CONCLUSIONS

The results reported in this work clearly demonstrate that the binding data of nanoMIPs cannot be conveniently described by simple models such as the Langmuir one but require more complex models that describe binding behaviors due to the presence of positive cooperativity in the interaction between binding sites and ligand molecules. The experimental results obtained with nanoMIPs with an increasing degree of cross-linking also indicate that such positive cooperativity could be dependent on the flexibility of the polymeric structure of nanoMIPs or, alternatively, on the presence of mutually close binding sites, an issue that certainly deserves further experimental investigation. In conclusion, it has been

https://doi.org/10.1021/acsapm.4c03726
ACS Appl. Polym. Mater. 2025, 7, 3286−3295

Table 2. Calculated Parameters ±1 Standard Error for Binding Isotherm Models Reported in Chart 1 and Considered in This Work[a]

	model	B_{max}		K_{eq}		N		m	
ciprofloxacin−nanoMIP 2%	Langmuir	11.56 ± 1.19	(9.70)	1.53 ± 0.24	(6.35)				
	Redlich-Peterson	10.58 ± 0.57	(18.53)	1.37 ± 0.06	(23.01)	2.43 ± 0.54	(4.48)		
	Toth	5.72 ± 0.40	(14.37)	2.51 ± 0.15	(16.80)	3.44 ± 1.14	(3.03)		
	Langmuir−Freundlich	6.59 ± 0.34	(19.37)	4.31 ± 0.36	(11.93)	1.57 ± 0.10	(15.4)		
	Generalized Freundlich	7.86 ± 0.36	(21.63)	11.10 ± 4.07	(2.72)	2.67 ± 0.68	(3.94)		
	Marczewski	6.91 ± 1.13	(6.13)	*5.27 ± 3.60*	*(1.46)*	1.36 ± 0.58	(2.36)	1.78 ± 0.74	(2.40)
ciprofloxacin−nanoMIP 10%	Langmuir	6.22 ± 0.23	(26.92)	10.72 ± 1.25	(8.58)				
	Redlich-Peterson	9.58 ± 0.37	(26.10)	4.15 ± 0.40	(10.35)	1.50 ± 0.10	(14.67)		
	Toth	5.09 ± 0.08	(64.08)	6.90 ± 0.28	(24.82)	2.88 ± 0.41	(7.03)		
	Langmuir−Freundlich	5.24 ± 0.07	(77.88)	13.12 ± 0.32	(41.06)	1.82 ± 0.09	(21.23)		
	Generalized Freundlich	5.98 ± 0.14	(42.31)	*81.59 ± 40.15*	*(2.03)*	5.48 ± 2.33	(2.36)		
	Marczewski	5.22 ± 0.10	(51.65)	12.10 ± 3.44	(3.52)	1.90 ± 0.31	(6.17)	1.70 ± 0.41	(4.10)
ciprofloxacin−nanoMIP 20%	Langmuir	*40.19 ± 55.43*	*(0.73)*	*0.14 ± 0.21*	*(0.69)*				
	Redlich-Peterson	3.39 ± 0.62	(5.49)	1.68 ± 0.28	(6.03)	*9.71 ± 8.25*	*(1.18)*		
	Toth	2.43 ± 0.15	(16.42)	2.35 ± 0.14	(16.25)	*17.70 ± 27.61*	*(0.64)*		
	Langmuir−Freundlich	3.26 ± 0.31	(10.61)	3.69 ± 0.42	(8.77)	1.96 ± 0.19	(10.49)		
	Generalized Freundlich	4.78 ± 0.56	(8.50)	*11.25 ± 8.33*	*(1.35)*	*3.85 ± 2.05*	*(1.88)*		
	Marczewski	2.55 ± 0.21	(12.04)	2.77 ± 0.20	(13.97)	*5.19 ± 2.82*	*(1.84)*	1.39 ± 0.15	(9.12)

[a] B_{max}: binding site concentration (nmol of binding sites × g of glass support); K_{eq}: apparent equilibrium binding constant (10^6 mol L^{-1}); and n,m: heterogeneity parameters. In parentheses: t-value at p = 0.05, values in italic indicate a probability $p > 0.05$ that the calculated parameter cannot be used to predict the values of the dependent variable (null hypothesis).

https://doi.org/10.1021/acsapm.4c03726
ACS Appl. Polym. Mater. 2025, 7, 3286−3295

Table 3. Information Criteria Calculated for the Binding Isotherm Models[a]

	model	BIC	ΔBIC
ciprofloxacin−nanoMIP 2%	Langmuir	8.0	20.7
	Redlich-Peterson	−2.3	10.4
	Toth	−2.9	9.8
	Langmuir−Freundlich	−12.7	0
	Generalized Freundlich	−12.5	0.2
	Marczewski	−9.9	2.8
ciprofloxacin−nanoMIP 10%	Langmuir	25.9	44.9
	Redlich-Peterson	1.4	20.4
	Toth	−6.7	12.2
	Langmuir−Freundlich	−19.0	0
	Generalized Freundlich	1.2	20.1
	Marczewski	−15.8	3.2
ciprofloxacin−nanoMIP 20%	Langmuir	−7.7	19.5
	Redlich-Peterson	−11.4	15.7
	Toth	−11.9	15.3
	Langmuir−Freundlich	−27.2	0
	Generalized Freundlich	−23.7	3.4
	Marczewski	−26.8	0.4

[a]BIC: Bayesian information criterion. ΔBIC: difference between the most negative BIC value (best model) and the other BIC values.

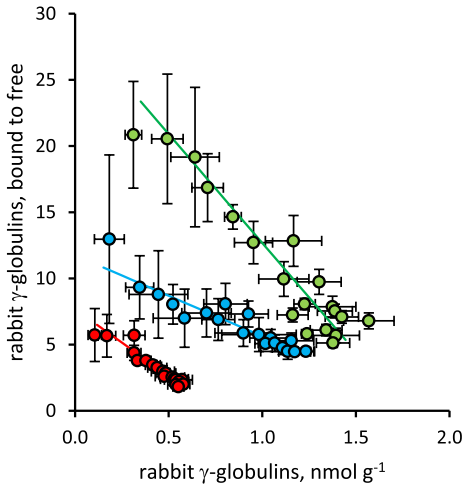

Figure 5. Scatchard plots for rabbit γ-globulins-binding nanoMIP 2% (red), nanoMIP 10% (green), and nanoMIP 20% (blue). Bound γ-globulins must be intended as nmol × g of glass beads. Original data taken from ref 43.

experimentally demonstrated for the first time that there is a substantial difference in binding behavior between antibodies of natural origin and the so-called "plastibodies" based on the molecular template, a difference whose implications for potential analytical applications such as nanoMIP-based sensors and immunoanalytical-like assays will have to be carefully considered.

■ ASSOCIATED CONTENT

Supporting Information

The Supporting Information is available free of charge at https://pubs.acs.org/doi/10.1021/acsapm.4c03726.

Calculation of free fraction, *F*, bound fraction, *B*, and ratio *B*/*F* and calculation on the mean distance of binding sites in nanoMIPs supported onto the surface of Spheriglass-2429 glass beads (PDF)

■ AUTHOR INFORMATION

Corresponding Author

Claudio Baggiani − *Laboratory of BioAnalytical Chemistry, Department of Chemistry, University of Torino, 10125 Torino, Italy*; orcid.org/0000-0003-1024-2532; Email: claudio.baggiani@unito.it

Authors

Valentina Testa − *Laboratory of BioAnalytical Chemistry, Department of Chemistry, University of Torino, 10125 Torino, Italy*

Laura Anfossi − *Laboratory of BioAnalytical Chemistry, Department of Chemistry, University of Torino, 10125 Torino, Italy*; orcid.org/0000-0002-2920-0140

Simone Cavalera − *Laboratory of BioAnalytical Chemistry, Department of Chemistry, University of Torino, 10125 Torino, Italy*; orcid.org/0000-0002-5353-647X

Fabio Di Nardo − *Laboratory of BioAnalytical Chemistry, Department of Chemistry, University of Torino, 10125 Torino, Italy*; orcid.org/0000-0003-0497-4251

Thea Serra − *Laboratory of BioAnalytical Chemistry, Department of Chemistry, University of Torino, 10125 Torino, Italy*

Complete contact information is available at: https://pubs.acs.org/10.1021/acsapm.4c03726

Author Contributions

Valentina Testa: methodology, investigation, and data analysis. Laura Anfossi: formal analysis and review. Simone Cavalera: review and editing. Fabio Di Nardo: writing original draft and editing. Thea Serra: investigation and data analysis. Claudio Baggiani: conceptualization, methodology, and writing original draft. All authors have read and agreed to the published version of the manuscript. All authors have given approval to the final version of the manuscript.

Notes

The authors declare no competing financial interest.

■ ACKNOWLEDGMENTS

Authors acknowledge support from the Project CH4.0 under the MUR program "Dipartimenti di Eccellenza 2023-2027" (CUP: D13C22003520001).

■ REFERENCES

(1) Chen, L.; Wang, X.; Lu, W.; Wu, X.; Li, J. Molecular Imprinting: Perspectives and Applications. *Chem. Soc. Rev.* **2016**, *45*, 2137−2211.

(2) Han, Y.; Tao, J.; Ali, N.; Khan, A.; Malik, S.; Khan, H.; Yu, C.; Yang, Y.; Bilal, M.; Mohamed, A. A. Molecularly Imprinted Polymers as the Epitome of Excellence in Multiple Fields. *Eur. Polym. J.* **2022**, *179*, 111582.

(3) Vlatakis, G.; Andersson, L. I.; Müller, R.; Mosbach, K. Drug Assay Using Antibody Mimics Made by Molecular Imprinting. *Nature* **1993**, *361*, 645−647.

(4) Wulff, G. Molecular Imprinting in Cross-Linked Materials with the Aid of Molecular Templates - A Way Towards Artificial Antibodies. *Angew. Chem., Int. Ed.* **1995**, *34*, 1812−1832.

(5) Mahon, C. S.; Fulton, D. A. Mimicking Nature with Synthetic Macromolecules Capable of Recognition. *Nat. Chem.* **2014**, *6*, 665−672.

(6) Hoshino, Y.; Shea, K. J. The Evolution of Plastic Antibodies. *J. Mater. Chem.* **2011**, *21*, 3517−3521.

(7) Garcia-Calzon, J. A.; Diaz-Garcia, M. E. Characterization of Binding Sites in Molecularly Imprinted Polymers. *Sens. Actuators, B* **2007**, *123*, 1180−1194.

(8) Lee, W.-C.; Cheng, C.-H.; Pan, H.-H.; Chung, T.-H.; Hwang, C. C. Chromatographic Characterization of Molecularly Imprinted Polymers. *Anal. Bioanal. Chem.* **2008**, *390*, 1101−1109.
(9) Umpleby, R. J.; Bode, M.; Shimizu, K. D. Measurement of the Continuous Distribution of Binding Sites in Molecularly Imprinted Polymers. *Analyst* **2000**, *125*, 1261−1265.
(10) Schauperl, M.; Lewis, D. W. Probing the Structural and Binding Mechanism Heterogeneity of Molecularly Imprinted Polymers. *J. Phys. Chem. B* **2015**, *119*, 563−571.
(11) Sips, R. On the Structure of a Catalyst Surface. *J. Chem. Phys.* **1948**, *16*, 490−495.
(12) Umpleby II, R. J.; Baxter, S. J.; Chen, Y.; Shah, R. N.; Shimizu, K. D. Characterization of Molecularly Imprinted Polymers with the Langmuir-Freundlich Isotherm. *Anal. Chem.* **2001**, *73*, 4584−4591.
(13) Ansell, R. J. Characterization of the Binding Properties of Molecularly Imprinted Polymers. *Adv. Biochem. Eng. Biotechnol.* **2015**, *150*, 51−93.
(14) Hill, A. V. A New Mathematical Treatment of Changes of Ionic Concentration in Muscle and Nerve under the Action of Electric Currents, with a Theory as to Their Mode of Excitation. *J. Physiol.* **1910**, *40*, 190−224.
(15) Perlmutter-Hayman, B. Cooperative Binding to Macromolecules. A Formal Approach. *Acc. Chem. Res.* **1986**, *19*, 90−96.
(16) Yang, D.; Kroe-Barrett, R.; Singh, S.; Roberts, C. J.; Laue, T. M. IgG Cooperativity − Is there Allostery? Implications for Antibody Functions and Therapeutic Antibody Development. *mAbs* **2017**, *9*, 1231−1252.
(17) Pap, T.; Horvai, G. Characterization of the Selectivity of a Phenytoin Imprinted Polymer. *J. Chromatogr. A* **2004**, *1034*, 99−107.
(18) Kirsch, N.; Alexander, C.; Davies, S.; Whitcombe, M. J. Sacrificial Spacer and Non-Covalent Routes toward the Molecular Imprinting of "Poorly-Functionalized" N-Heterocycles. *Anal. Chim. Acta* **2004**, *504*, 63−71.
(19) Syu, M.-J.; Nia, Y.-M. An Allosteric Model for the Binding of Bilirubin to the Bilirubin Imprinted Poly(Methacrylic Acid-co-Ethylene Glycol Dimethylacrylate). *Anal. Chim. Acta* **2005**, *539*, 97−106.
(20) Mueller, A. A. Note about Crosslinking Density in Imprinting Polymerization. *Molecules* **2021**, *26* (5139), 5139.
(21) Haupt, K.; Rangel, P. X. M.; Bui, B. T. S. Molecularly Imprinted Polymers: Antibody Mimics for Bioimaging and Therapy. *Chem. Rev.* **2020**, *120*, 9554−9582.
(22) Xu, S.; Wang, L.; Liu, Z. Molecularly Imprinted Polymer Nanoparticles: An Emerging Versatile Platform for Cancer Therapy. *Angew. Chem., Int. Ed.* **2021**, *60*, 3858−3869.
(23) Silva, A. T.; Figueiredo, R.; Azenha, M.; Jorge, P. A. S.; Pereira, C. M.; Ribeiro, J. A. Imprinted Hydrogel Nanoparticles for Protein Biosensing: A Review. *ACS Sens.* **2023**, *8*, 2898−2920.
(24) Hoshino, Y.; Kodama, T.; Okahata, Y.; Shea, K. J. Peptide Imprinted Polymer Nanoparticles: A Plastic Antibody. *J. Am. Chem. Soc.* **2008**, *130*, 15242−15243.
(25) Poma, A.; Guerreiro, A.; Whitcombe, M. J.; Piletska, E. V.; Turner, A. P.; Piletsky, S. A. Solid-Phase Synthesis of Molecularly Imprinted Polymer Nanoparticles with a Reusable Template - "Plastic Antibodies. *Adv. Funct. Mater.* **2013**, *23*, 2821−2827.
(26) Ambrosini, S.; Beyazit, S.; Haupt, K.; Tse Sum Bui, B. Solid-Phase Synthesis of Molecularly Imprinted Nanoparticles for Protein Recognition. *Chem. Commun.* **2013**, *49*, 6746−6748.
(27) Harrison, F.; Katti, S. K. Hazards of Linearization of Langmuir's Model. *Chemometr. Intell. Lab. Syst.* **1990**, *9*, 249−255.
(28) Bolster, C. H.; Hornberger, G. M. On the Use of Linearized Langmuir Equations. *Soil Sci. Soc. Am. J.* **2008**, *72*, 1848.
(29) Osmari, T. A.; Gallon, R.; Schwaab, M.; Barbosa-Coutinho, E.; Severo, J. B., Jr; Pinto, J. C. Statistical Analysis of Linear and Non-Linear Regression for the Estimation of Adsorption Isotherm Parameters. *Adv. Sci. Technol.* **2013**, *31*, 433−458.
(30) Buttersack, C. Modeling of Type IV and V Sigmoidal Adsorption Isotherms. *Phys. Chem. Chem. Phys.* **2019**, *21*, 5614−5626.
(31) Klotz, I. M. Ligand-Receptor Complexes: Origin and Development of the Concept. *J. Biol. Chem.* **2004**, *279*, 1−12.
(32) Brouers, F. Statistical Foundation of Empirical Isotherms. *Open J. Statistics* **2014**, *04*, 687−701.
(33) Marczewski, A. W.; Jaroniec, M. New Isotherm Equation for Single-Solute Adsorption from Dilute Solutions on Energetically Heterogeneous Solids. *Monatsh. Chem.* **1983**, *114*, 711−715.
(34) Langmuir, I. The Adsorption of Gases on Plane Surfaces of Glass, Mica, and Platinum. *J. Am. Chem. Soc.* **1918**, *40*, 1361−1403.
(35) Chu, K. H.; Hashim, M. A.; Santos, Y. T. d. C.; Debord, J.; Harel, M.; Bollinger, J. C. The Redlich−Peterson Isotherm for Aqueous Phase Adsorption: Pitfalls in Data Analysis and Interpretation. *Chem. Eng. Sci.* **2024**, *285*, 119573.
(36) Sips, R. On the Structure of a Catalyst Surface, II. *J. Chem. Phys.* **1950**, *18*, 1024−1026.
(37) Toth, J. Thermodynamical Correctness of Gas/Solid Adsorption Isotherm Equations. *J. Colloid Interface Sci.* **1994**, *163*, 299−302.
(38) Cavalera, S.; Chiarello, M.; Di Nardo, F.; Anfossi, L.; Baggiani, C. Effect of Experimental Conditions on the Binding Abilities of Ciprofloxacin-Imprinted Nanoparticles Prepared by Solid-Phase Synthesis. *React. Funct. Polym.* **2021**, *163*, 104893.
(39) Chiarello, M.; Anfossi, L.; Cavalera, S.; Di Nardo, F.; Artusio, F.; Pisano, R.; Baggiani, C. Effect of Polymerization Time on the Binding Properties of Ciprofloxacin-Imprinted nanoMIPs Prepared by Solid Phase Synthesis. *Polymers* **2021**, *13*, 2656.
(40) Allen, D. M. The Relationship Between Variable Selection and Data Agumentation and a Method for Prediction. *Technometrics* **1974**, *16*, 125−127.
(41) Cavanaugh, J. E.; Neath, A. A. The Bayesian Information Criterion: Background, Derivation, and Applications. *WIREs Comput. Stat.* **2012**, *4*, 199−203.
(42) Kass, R. E.; Raftery, A. E. Bayes Factors. *J. Am. Stat. Assoc.* **1995**, *90*, 773−795.
(43) Testa, V.; Anfossi, L.; Cavalera, S.; Di Nardo, F.; Serra, T.; Baggiani, C. The Amount of Cross-Linker Influences Affinity and Selectivity of nanoMIPs Prepared by Solid-Phase Polymerization Synthesis. *Polymers* **2024**, *16* (532), 532.

https://doi.org/10.1021/acsapm.4c03726
ACS Appl. Polym. Mater. 2025, 7, 3286−3295